FEDER, M. 1976. Lunglessness, body size, and metabolic rate in salamanders. Physiol. Zool. 49:398–406.
FINKLER, M. S., M. T. SUGALSKI, D. L. CLAUSSEN, AND S. J. BEAUPRE. 2003. Sex-related differences in metabolic rate and locomotor performance in breeding spotted salamanders (*Ambystoma maculatum*). Copeia. 2003:887–893.
FORD, N. B., AND G. A. SHUTTLESWORTH. 1986. Effects of variation in food intake on locomotory performance of juvenile garter snakes. Copeia 1986:999–1001.
GARLAND, T., JR., AND S. J. ARNOLD. 1983. Effects of a full stomach on locomotory performance of juvenile garter snakes (*Thamnophis elegans*). Copeia 1983:1092–1096.
HILLMAN, S. S., R. C. DREWES, M. S. HEDRICK, AND T. V. HANCOCK. 2014. Physiological vagility: correlations with dispersal and population genetic structure of amphibians. Physiol. Biochem. Zool. 87:105–112.
IBM CORP. 2013. IBM SPSS Statistics for Windows, Version 22.0. IBM Corp., Armonk, New York.
JOHNSON, J. R., B. B. JOHNSON, AND H. B. SHAFFER. 2010. Genotype and temperature affect locomotor performance in a tiger salamander hybrid swarm. Funct. Ecol. 24:1073–1080.
KIESECKER, J. M., A. R. BLAUSTEIN, AND L. K. BELDEN. 2001. Complex causes of amphibian population declines. Nature 410:681–684.
LINDQUIST, S. B., AND M. D. BACHMANN. 1980. Feeding behavior of the tiger salamander, *Ambystoma tigrinum*. Herpetologica 36:144–158.
MARSH, D. M., K. A. THAKUR, K. C. BULKA, AND L. B. CLARKE. 2004. Dispersal and colonization through open fields by a terrestrial, woodland salamander. Ecology 85:3396–3405.
MEHTA, R. S. 2006. Meal size effects on antipredator behavior of hatchling trinket snakes, *Elaphe helena*. Ethology 112:649–656.
MILANOVICH J. R., W. E. PETERMAN, N. P. NIBBELINK, AND J. C. MAERZ. 2010. Projected loss of a salamander hotspot as a consequence of projected global climate change. PLOS ONE 5:e12189.
PETRANKA, J. W. 2010. Salamanders of the United States and Canada. 2nd ed. Smithsonian Institution, Washington, District of Columbia. 587 pp.
PINCHEIRA-DONOSO, D., D. J. HODGSON, AND T. TREGENZA. 2008. The evolution of body size under environmental gradients in ectotherms: why should Bergmann's rule apply to lizards? BMC Evol. Biol. 8:68.
PLUMMER, M. V. 1997. Speed and endurance of gravid and nongravid green snakes, *Opheodrys aestivus*. Copeia 1997:191–194.
SCHALK, C. M., AND T. M. LUHRING. 2010. Vagility of aquatic salamanders: implications for wetland connectivity. J. Herpetol. 44:104–109.
SIH, A., AND B. CHRISTENSEN. 2001. Optimal diet theory: when does it work, and when and why does it fail? Anim. Behav. 61:379–390.
TRENHAM, P. C., H. B. SHAFFER, W. D. KOENIG, AND M. R. STROMBERG. 2000. Life history and demographic variation in the California tiger salamander (*Ambystoma californiense*). Copeia 2000:365–377.
———, W. D. KOENIG, AND H. B. SHAFFER. 2001. Spatially autocorrelated demography and interpond dispersal in the salamander *Ambystoma californiense*. Ecology 82:3519–3530.
WALSTON, L. J., AND S. J. MULLIN. 2005. Evaluation of a new method for measuring salamanders. Herpetol. Rev. 36:290–292.
WHITEMAN, H. H., S. A. WISSINGER, AND A. J. BOHONAK. 1994. Seasonal movement patterns in a subalpine population of the tiger salamander, *Ambystoma tigrinum nebulosum*. Can. J. Zool. 72:1780–1787.

Herpetological Review, 2016, 47(4), 586–591.

Theory and Practice of the Hydrodynamic Redesign of Artificial Hellbender Habitat

The Hellbender (*Cryptobranchus alleganiensis*) is a cryptic, large-bodied amphibian endemic to cool Appalachian and Ozark mountain streams (Nickerson and Mays 1973; Petranka 1998). As is the case with many salamanders, a long lifespan, reliance on aquatic habitat and sensitivity to environmental change make *C. alleganiensis* an excellent indicator of ecosystem health (Olson et al. 2012; Welsh and Ollivier 1998). Unfortunately, these same qualities have led to drastic declines in populations of these amphibians nearly ubiquitously across their range (Nickerson and Mays 1973; Wheeler et al. 2003). As a result, the Ozark subspieces, *C. a. bishopi*, was listed under the U.S. Endangered Species Act as Endangered in 2011 (Federal Register 2011), and has been deemed Imperiled (N2) by NatureServe (2015). The eastern subspecies, *C. a. alleganiensis*, has been listed due to varying degrees of risk in 13 of the 16 states in which it occurs (Mayasich et al. 2003; KDFWR 2013), and has been assigned a national NatureServe (2015) status of Vulnerable to Apparently Secure (N3/N4). As a species, *C. alleganiensis* is considered Near Threatened by the International Union for Conservation of Nature (IUCN; Hammerson and Phillips 2004).

MOHAMMED G. MOHAMMED
Department of Civil and Environmental Engineering, University of Missouri, Columbia, Missouri 65201, USA
e-mail: mgm7fc@mail.missouri.edu
ARIANNE F. MESSERMAN
Division of Biological Sciences, University of Missouri, Columbia, Missouri 65201, USA
e-mail: afmxw7@mail.missouri.edu
BRYAN D. MAYHAN
Department of Civil and Environmental Engineering and Geographic Resources Center, University of Missouri, Columbia, Missouri 65201, USA
e-mail: mayhanb@missouri.edu
KATHLEEN M. TRAUTH
Department of Civil and Environmental Engineering, University of Missouri, Columbia, Missouri 65201, USA
e-mail: trauthk@missouri.edu

Habitat loss due to increased sedimentation from development within inhabited watersheds is suspected as a leading cause of declines among *C. alleganiensis* populations (Wheeler et al. 2003). Large loads of particulate matter entering streams deplete dissolved oxygen levels and fill the concave undersides of the large, flat rocks that serve as shelter and nesting sites for *C. alleganiensis*. In combination, these effects can reduce animal fitness and lead to breeding failure (Ringler and Hall 1975; Harlan and Wilkinson 1981; Briggler and Ackerson 2012; Browne et al. 2012). To combat this landscape-level threat to *C. alleganiensis*, Briggler and Ackerson (2012) developed artificial nesting structures to increase Hellbender habitat while reducing sediment accumulation. Wild *C. alleganiensis* adults have inhabited and successfully bred in these boot-shaped nest boxes within Missouri streams.

The success of nest boxes in Missouri led researchers to test whether similar management tools could increase *C. a. alleganiensis* populations in the streams of western North Carolina, where these salamanders are listed as a Species of Special Concern (Messerman 2014). Fifty-four nest boxes were constructed following the boot-shaped design of Briggler and Ackerson (2012) in May 2013, and were installed across five known *C. alleganiensis* stream sites between late June and early August 2013. Messerman (2014) then monitored each nest box every three to four weeks through November 2013, and the boxes were revisited in August 2014 and July 2015 to observe structural condition and occupancy (Messerman, pers. obs.). Of the 54 nest boxes, only two structures at a single site were confirmed as inhabited in 2014 and 2015, and no breeding events were detected (Messerman, pers. obs.). Moreover, many of these ~50 lb concrete boxes moved in flood events or accumulated sediment at the downstream tunnel entrance (Messerman 2014). The low success of the boot-shaped nest box design in North Carolina may be attributed to the sites generally being narrower and shallower than those in Missouri, with much of the substrate consisting of bedrock slabs covered by relatively thin layers of rock, gravel and silt. Here we address the observed shortcomings of the original North Carolina design through the lens of engineering, and present a new and easily implemented nest box model for use in streams like those found in western North Carolina.

Flow Considerations

The two issues of sedimentation and disturbance/movement of the nest boxes can be addressed by a consideration of flow in the vicinity of a solid object. Such an object can cause changes in the flow velocity and pressure. These changes can be described using several equations. The first equation of interest is the continuity equation that represents the conservation of mass between a point 1 and a point 2 which are two cross sections along a stream:

$$Q = \rho_1 A_1 V_1 = \rho_2 A_2 V_2$$

where Q is the flow or discharge (volume per time), ρ is the density of the fluid (mass per volume), A is the cross-sectional area of flow (length squared) and V is the velocity of flow (length per time). Continuity states that the mass flowing into a designated volume must equal the mass flowing out of the volume. For a fluid of essentially constant density (e.g., water), where $\rho_1 = \rho_2$, the equation reduces to the product of area and velocity being constant. Thus, if the cross-sectional area is increased, the velocity will decrease, and vice versa.

Flow is also governed by the Bernoulli equation, where the total energy of flow, H (length), has components of pressure, P (force per area), depth, y (length) and velocity. The difference in energy states between a point 1 and a point 2 can thus be represented by:

$$H_1 = \frac{P_1}{\gamma} + y_1 + \frac{V_1^2}{2g} = \frac{P_2}{\gamma} + y_2 + \frac{V_2^2}{2g} + h_L = H_2$$

where γ is the specific weight of the fluid (force per volume), g is the gravitational constant (length per time squared) and h_L represents the energy lost in the flow between the two points. As a fluid flows from point 1 to point 2, the distribution of energy between the components may change. As an example, water flowing in a water main may sometimes have more of its energy in terms of velocity, and at other times may have more of its energy in terms of water pressure. For ease of conversion between the components, the energy terms are all expressed in units of length.

Another useful concept to consider is that of streamlines. Streamlines depict velocity vectors (magnitude and direction), and their orientation is always parallel to the direction of flow. With localized disruptions to flow, as with the placement of a

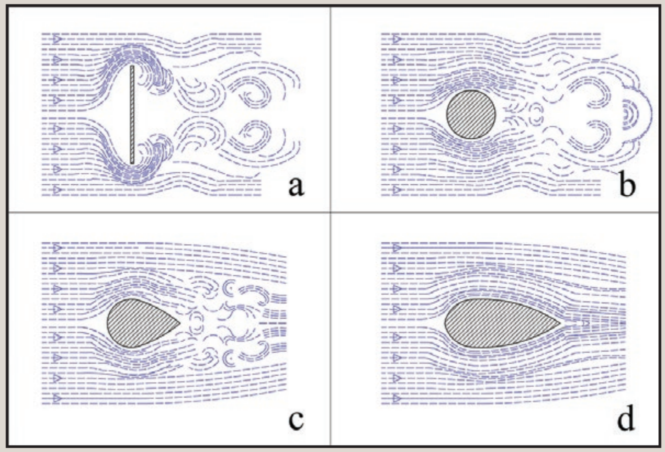

Fig. 1. The impact of object shape on the production of eddy currents downstream of an object (based on Richter and Nikrityuk [2012]).

Body (Flow From left to right)	L/d	Re= V d/v	C_D
Bodies of revolution			
1) Sphere: D		10^5 $>3 \times 10^5$	0.50 0.20
2) Ellipsoid : d= 1, 2		$>2 \times 10^5$	0.07
3) Circular cylinder axis vertical to follow: L, d	1 5 20 ∞ 5 ∞	10^5 $>5 \times 10^5$ 	0.63 0.74 0.90 1.20 0.35 0.33
4) Rectangular plate: L=length d= width	1 5 20 ∞	$>10^3$	1.16 1.20 1.50 1.90
5) Square cylinder: d		3.5×10^4 10^4-10^5	2.0 1.6

Fig. 2. Drag coefficients for different shapes and dimensions (based on Prasuhn [1980]).

Table 1. Standard coefficients of friction for materials in contact with concrete.

Contacting Surfaces	Friction Coefficient (µf)
Concrete on soil/rock	0.30
Concrete on steel	0.45
Cement Blocks on cement blocks	0.65
Cement Concrete on dry clay	0.40
Cement Concrete on wet clay	0.20
Cement Concrete on wet sand	0.40
Cement Concrete on dry sand	0.50–0.60
Cement Concrete on dry gravel	0.50–0.60
Cement Concrete on dry rock	0.60–0.70
Cement Concrete on wet rock	0.50

Note: Friction is greater on dry surfaces than wet surfaces.

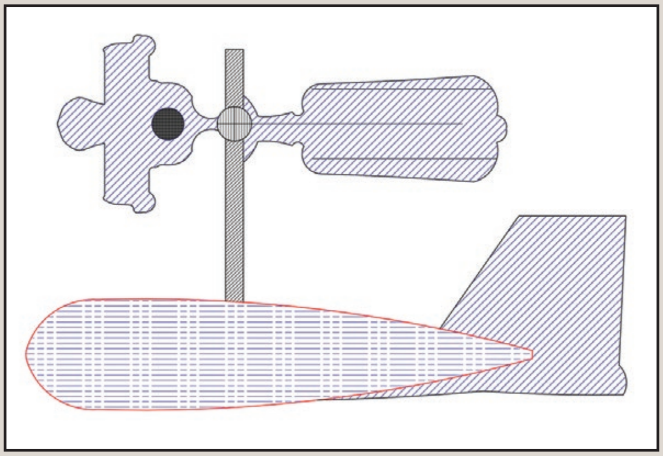

Fig. 3. Streamlined shape of a current meter (based on Prasuhn [1980]).

solid object in the flow, the streamlines are disrupted. Streamlines in the flow as a whole (e.g., a river) may be undisturbed and remain constant, but streamlines immediately surrounding the object will be compressed (Fig. 1). What appears as a dark area in Fig. 1 is the result of the streamlines being compressed. The compression of the streamlines can be seen as decreasing the cross-sectional area of flow associated with each streamline. By continuity, and because the amount of flow is not decreasing just because an object has been placed in the stream, a decrease in the cross-sectional area of flow will be associated with an increase in the velocity. By Bernoulli's equation, an increase in velocity will be associated with a decrease in the pressure of the flow in the vicinity of the solid object.

The low-pressure area is located near the rear portion (i.e., downstream region) of the hydraulic structure, and this difference in pressures gives rise to what is called form drag, where drag is used to indicate a resistance to flow as represented by a force. The shape and relative dimensions of the object will impact the form drag that results from flow. Drag can also be thought of as the impact of flowing water on a solid body. Flow may thus exert a force on a solid body as represented by:

$$F_D = C_D A \frac{\rho V_0^2}{2}$$

where F_D is the drag force, C_D is the drag coefficient associated with the shape and dimensions of the solid object, A is the cross-sectional area that is projected upstream by the object (length squared), ρ is the density of the fluid and V_0 is the flow velocity upstream of the solid object. Over time, experiments measuring the impact of flow around solid bodies have resulted in an accepted set of drag coefficients associated with different shapes and relative dimensions (Fig. 2). As can be seen, drag coefficients can vary from 0.07 to 2.00, thus greatly impacting the drag force that flowing water will exert on a solid body. Drag coefficients may also be impacted based upon the values of the dimensionless Reynolds number (**Re**) (Fig. 2), where larger **Re** are associated with decreased drag based upon achieving a fully rough condition. The value for the **Re** is calculated as:

$$Re = \frac{Vd}{\nu}$$

where V is the velocity of the flow, d is the diameter of a pipe or can be considered as a depth of flow and ν is the kinematic viscosity of the fluid (length squared per time). The **Re** will be large if the velocity and/or diameter are large or if the kinematic viscosity is small.

The movement of fluid around the solid object means that ordered streamlines are absent from the area immediately downstream of the object, producing an area of disordered flow. In this disordered flow, the velocity vectors occur in all directions and may be circular in motion, where they are called eddies (Fig. 1a, b, and c). Parcels of water moving in opposite directions and impacting each other result in water with reduced velocities. These reduced velocities have less energy and are thus unable to transport the existing sediment load. Sedimentation may thus occur downstream of a solid object.

In order for an object (that is not buoyant) lying flat on a surface to be moved by the water flowing around it, the drag force must be greater than the resisting force, that is, the force required to initiate sliding motion. The resistance to the initiation of sliding motion is based on friction, where a friction force, F_f can be calculated as:

$$F_f = \mu W$$

where µ is the coefficient of friction based upon the two materials coming in contact with each other (Table 1) and W is the weight of the object that may be moved.

Engineering Issues with Rectangular Nest Box

Knowing from the above discussion that object shape and relative dimensions impact flow parameters, it is possible to assign at least partial causes to the problems reported with the operation of rectangular nest boxes. Sedimentation of suspended materials along the downstream face of the rectangular nest boxes could be attributed to disordered flow where velocity vectors are oriented in all directions, including some that are in opposite directions that negate each other, resulting in low velocities. Reduced velocities allow suspended sediment to drop out. The movement of the nest boxes from their original locations could be attributed to drag forces that are initiated on the upstream side of the nest box as the flow must be redirected around it. Drag forces are greater from larger, faster, storm flows, and it may be during these times that the disturbance occurs. Thus, there are design issues with both the upstream and downstream

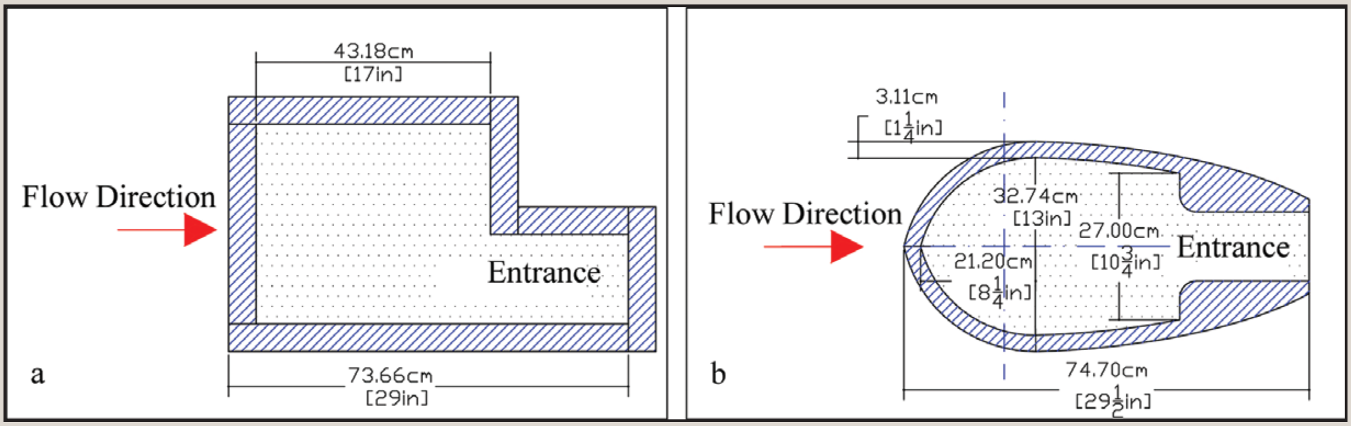

Fig. 4. a. Top view of existing nest box shape (rectangular); b. Top view of redesigned nest box shape (streamlined).

faces of the nest box that must be addressed simultaneously. An alternative nest box design is proposed that is evaluated based upon the fluid mechanics principles discussed above.

Engineering Constraints with Nest Box Redesign

There are a number of constraints that are imposed on the redesign process based on the fact that the nest boxes are being utilized as breeding locations for Hellbenders in their natural habitat.

1. There must be an internal cavity that is large enough for the male Hellbender to move in along with any egg masses present.
2. While the eggs are developing, the male needs to be able to defend them from predators, so a tunnel (length greater than width) entrance is desired that provides only limited access to the internal cavity.
3. Consistent with natural habitat, the entrance to the internal cavity must be located on the downstream side of the nest box (Pfingsten and Downs 1989).
4. To reduce the effects of human disturbance on Hellbenders, the nest boxes must be placed far away from roads and other easy access points. Thus, the structures must be light enough to be carried to more remote locations in the field by researchers.
5. The bottom of the nest box must be essentially flat in order to be stable in its placement on the bottom of a stream bed.
6. Any new nest boxes must be able to be constructed from an inexpensive material and with a design that limits constructability and durability issues.

Modifications to Nest Box Design

Given the above constraints, the design challenge was to develop a nest box to meet the required characteristics for biological functionality while improving hydrodynamic performance. Hydrodynamics can provide examples of solid objects designed to be placed in flowing water with the intention of causing the least disturbance. Once such example consists of the weights that are used with current meters (Fig. 3), devices utilized to measure the velocity of flow at different depths within a stream, based upon the rate of rotation of a set of vanes. Weights are used to orient the flow measuring device in a vertical position to reduce reading errors caused from velocity vectors that are not perpendicular to the axis holding the rotating vanes. The shape of the weight is established both to minimize the drag on the weight that would cause it to move away from the vertical and to minimize the disordered downstream flow that could produce velocity vectors in multiple directions.

Computer-aided design software (AutoCAD, Autodesk, Inc., 2015) was utilized to produce the redesigned Hellbender nest box. Relative dimensions were identified from a drawing of a current meter weight and manipulated to incorporate all of the nest box design constraints. The streamlined nest box has a different external shape and interior space in comparison to the original rectangular design (Fig. 4).

The upstream projection of the current meter weight is a rounded point, approximating a parabolic curve. Producing forms for a pointed projection can be difficult and may not allow for sufficient concrete thickness or wire reinforcement. Additionally, points can be problematic as they may be subject to breakage from the impact of transported rocks/cobbles. The current meter weight is three-dimensional and is considered to be a rotational body, meaning that if the direction of flow is considered as the x-axis, then the body has the same curvature in the y–z plane. The fact that the nest box must be flat on the bottom means that the rotational body must be truncated on the bottom. Thus, for the redesigned nest box, the upstream parabolic projection was flattened for constructability and durability, and the shape of the nest box mimics only the upper half of the current meter weight shape.

The rear portion of the current meter weight decreases dramatically and finishes with the addition of fins that help to properly orient the weight with respect to the oncoming flow. Fins are not necessary for the performance of the nest box and were never considered. The significant decrease in the rear projected area had to be modified in order to accommodate the placement of the access tunnel, which was then subsumed into the body of the nest box. Thus, the decreasing portion of the rear projection was truncated and has relative dimensions that are more consistent with the middle portion of the current meter weight. The streamlined shape of the current meter weight helps to direct the streamlines around the body so that they may rejoin together downstream of the body, in order that any eddies of disordered flow that might induce sedimentation occur downstream of the body. Without disordered flow, velocities are maintained to keep sediment in suspension.

Table 2. Initiation of motion calculations for rectangular and streamlined nest boxes.

Flow velocity V (m/s)	Rectangular Nest Box					Streamlined Nest Box				
	C_{D1}	A_1 (m^2)	F_{D1} (N)	F_{F1} (N)	Sliding Force = F_{D1} - F_{F1}	C_{D2}	A_2 (m^2)	F^{D2} (N)	FF2 (N)	Sliding Force = F_{D2} - F_{F2}
0.1	2	0.06	0.56	86.66	-86.10	0.10	0.07	0.03	118.81	-118.77
0.5	2	0.06	14.00	86.66	-72.66	0.10	0.07	0.86	118.81	-117.95
1	2	0.06	56.00	86.66	-30.66	0.10	0.07	3.45	118.81	-115.36
1.25	2	0.06	87.50	86.66	0.84	0.10	0.07	5.39	118.81	-113.42
1.86	2	0.06	193.74	86.66	107.08	0.10	0.07	11.94	118.81	-106.87
3	2	0.06	504.00	86.66	417.34	0.10	0.07	31.05	118.81	-87.76
5	2	0.06	1400.00	86.66	1313.34	0.10	0.07	86.25	118.81	-32.56
5.87	2	0.06	1931.81	86.66	1845.15	0.10	0.07	119.01	118.81	0.204

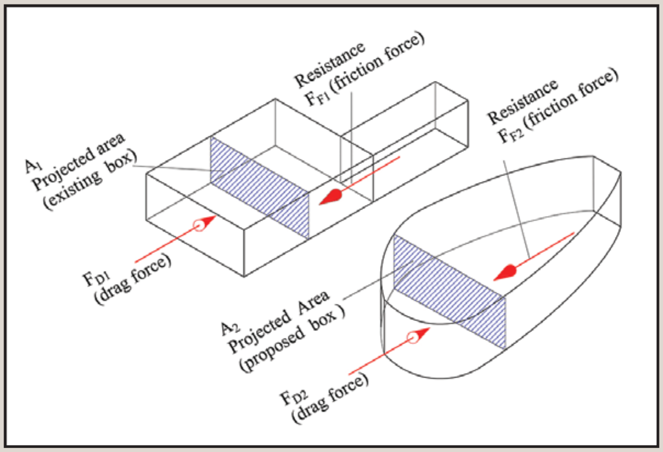

Fig. 5. Projected area and orientation of the drag and friction forces for the rectangular and streamlined shapes.

Fig. 6. Photographs of the streamlined nest box prototype.

The elongation of the nest box for both the upstream and downstream issues means that the weight of the box has increased beyond the approximately 50 lb of the nest boxes used previously in North Carolina. Because of the use of reinforcing wire mesh, the thickness of the walls was decreased to 1" to attempt to limit the increase in the weight. Additionally, the top was designed as a lid that could be carried into the field separately and would provide access to the nest box for visual inspection to verify usage/habitation.

Reduction in Drag Force for the Proposed Nest Box

To determine the potential impact of a redesigned streamlined nest box, a series of calculations were performed (not an actual test of motion) between the existing, rectangular nest box design and the hydrodynamically redesigned, streamlined nest box (Table 2). The calculations (for water with ρ = 1000 kg/m^3) are based on velocities that might be expected during periods of low flow and high flow (during storm events). The characteristics that would produce any given velocity are a function of the contributing watershed area, the design precipitation event, as well as the stream cross-section, surface roughness and slope. A drag coefficient for the projection of the rectangular nest box can safely be assumed to be 2.0 (Fig. 2). The shape of the redesigned nest box has no direct analog, so an approximation is made. The drag coefficient of 0.07 for a 2:1 ellipsoid may be too low, so a value of 0.10 was used for general comparison purposes. The area used in the drag calculations is the projected area (Fig. 5) that is larger for the hydrodynamic box (0.069 m^2) than for the rectangular box (0.056 m^2). A coefficient of friction of 0.3 was used as corresponding to a concrete box positioned on a soil/rock channel bottom. A weight of 222.4 N (50 lb) was used for the rectangular box, while a weight of 395.9 N (89 lb) was calculated from the design drawings for the streamlined box. Rocks placed on a nest box for camouflage would have a similar effect on stability for either a rectangular or a streamlined box, and were thus not incorporated into the calculations.

Motion begins once a drag force is greater than a resisting friction force. Given the assumptions above, the predictive calculations indicate that motion would be initiated for the rectangular box at a flow velocity of 1.25 m/s (4.10 ft/s), while motion would be predicted to be initiated for the streamlined box at a flow velocity of 5.87 m/s (19.25 ft/s). This is a more than a four-fold increase in the calculated velocity predicted to destabilize a nest box.

Construction Considerations

Once the design was completed, the form for pouring the streamlined nest box had to itself be designed. In order that the constructed prototype maintains a shape with specific hydrodynamic properties, the scale drawings from AutoCAD were transferred to multiple panels of plywood for cutting. Once cut, the plywood sheets that create the outside of the nest box were glued and screwed together to form a solid, durable and reusable outer mold. The interior surface was sanded and covered with a putty to ensure easy release of the nest box from the mold. As indicated earlier, the prototype needed a separate lid for easier transport. The lid mold includes an inner lip to allow the lid to sit smoothly and snugly upon placement in the field.

The requirement for an internal cavity necessitated a removable wooden piece that would establish the shape and size of the cavity. An interior mold was also created for the access tunnel. It was divided into three parts with the center being a wedge shape to facilitate tapping out and removal of the outer two sections.

Hardware cloth was utilized to reinforce the concrete, which for this initial prototype was simply the thinnest mortar commonly used for bonding ceramic tiles (QUIKRETE ®). All walls of the nest box were reinforced, with particular attention being given to the wrapping in the vicinity of the access tunnel. It is important to use a concrete containing sand, as a larger aggregate would make it difficult to adequately pour the thin walls of the structure and ensure complete contact between the cement and the aggregate. A constant moisture content between the several batches of concrete that were required to pour the entire nest box ensures a consistent strength between the batches. During the pour, a plastic hammer and a thin wooden shim were used to remove the air from the poured concrete, especially the walls, to improve strength. The molded concrete was wetted at least two times each day during curing, especially for the first seven days, to prevent cracking and facilitate the chemical reactions of the setting concrete. The concrete was allowed to set for 24 hours before removal from the mold, and continued to develop strength over time with continued wetting. Photographs show multiple views of the constructed nest box (Fig. 6).

Conclusions

Collaboration between a biologist and several engineers resulted in the redesign of a previously employed rectangular Hellbender nest box to meet biological requirements and improve field performance. Analyzing the functioning of the nest box from the perspective of hydrodynamics identified at least partial reasons for observed instability and sedimentation around the downstream access tunnel. The analysis further suggested how the redesign should be undertaken: producing modifications to the upstream face in order to reduce drag caused by flowing water and to the downstream face to complete the redirection of streamlines around the nest box to limit sedimentation. The more than four-fold increase in the predicted velocity of flow required to destabilize the streamlined nest box as compared to the rectangular nest box (as produced by demonstration calculations), suggests that it is a tool with a greater likelihood of success in augmenting Hellbender populations in North Carolina stream sites. At this time, researchers in North Carolina are in the process of building, installing and testing the efficacy of the redesigned nest box in the field. Results from the field testing will be incorporated into future refinement of the design.

Acknowledgments.—We thank Joseph J. Apodaca, John D. Groves, Benjamin G. Prater, Stephen F. Spear and Lori A. Williams for their support and valuable feedback.

Literature Cited

Briggler, J. T., and J. R. Ackerson. 2012. Construction and use of artificial shelters to supplement habitat for hellbenders (*Cryptobranchus alleganiensis*). Herpetol. Rev. 43:412–416.

Browne, R. K., H. Li, D. McGinnity, S. Okada, W. Zhenghuan, C. M, Bodinof, K. J. Irwin, A. McMillan, and J. T. Briggler. Survey techniques for giant salamanders of the aquatic Caudata. Amphib. Reptile. Conserv. 5:1–16.

USWFS (U.S. Fish and Wildlife Service). 2011. Endangered and threatened wildlife and plants: endangered status for the Ozark Hellbender Salamander. Federal Register 76:61956–61978.

Hammerson, G., and C. Phillips. 2004. *Cryptobranchus alleganiensis.* The IUCN Red List of Threatened Species 2004: e.T59077A11879843. Available at http://www.iucnredlist.org/details/full/59077/0. Archived by WebCite at http://www.webcitation.org/6h6kosDkm on 28 April 2016.

Harlan, R. A., and R. F. Wilkinson. 1981. The effects of progressive hypoxia and rocking activity on blood oxygen tension for hellbenders, *Cryptobranchus alleganiensis.* J. Herpetol. 1981:383–387.

KDFWR (Kentucky Department of Fish and Wildlife Resources). 2013. Kentucky's Comprehensive Wildlife Conservation Strategy. Available at http://fw.ky.gov/WAP/Pages/Default.aspx. Archived by WebCite at http://www.webcitation.org/6h44WGor9 on 26 April 2016.

Mayasich, J., D. Grandmaison, and C. Phillips. 2003. Eastern hellbender status assessment report. Natural Resources Research Institute, Technical Report 9:1–41.

Messerman, A. 2014. The use of nest boxes by the hellbender salamander in western North Carolina. Master's Thesis, Duke University, Durham, North Carolina.

NatureServe. 2015. NatureServe Explorer: An online encyclopedia of life [web application]. Version 7.1. Available at http://explorer.natureserve.org. Archived by WebCite at http://www.webcitation.org/6h44lA8ll on 26 April 2016.

Nickerson, M. A., and C. E. Mays. 1973. The Hellbenders: North American "Giant Salamander." Milwaukee Public Museum, Publications in Biology and Geology Number 1.

Olson, Z. H., J. T. Briggler, and R. N. Williams. 2012. An eDNA approach to detect eastern hellbenders (*Cryptobranchus a. alleganiensis*) using samples of water. Wildl. Res. 39:629–636.

Petranka, J. W. 1998. Salamanders of the United States and Canada. Smithsonian Institution Press, Washington, DC.

Pfingsten, R. A., and F. L. Downs. 1989. Salamanders of Ohio. Bulletin of the Ohio Biological Survey 7(2).

Prasuhn, A. L. 1980. Fundamentals of Fluid Mechanics. Prentice Hall, Englewood Cliffs, New Jersey.

Richter, A. and P. A. Nikrityuk. 2012. Drag forces and heat transfer coefficients for spherical, cuboidal and ellipsoidal particles in cross flow at sub-critical Reynolds numbers. Int. J. Heat Mass Tran. 55:1343–1354.

Ringler, N. H., and J. D. Hall. 1975. Effects of logging on water temperature, and dissolved oxygen in spawning beds. Trans. Am. Fish. Soc. 104:111–121.

Welsh, H. H., and L. M. Ollivier. 1998. Stream amphibians as indicators of ecosystem stress: a case study from California's redwoods. Ecol. Appl. 8:1118–1132.

Wheeler, B. A., E. Prosen, A. Mathis, and R. F. Wilkinson. 2003. Population declines of a long-lived salamander: a 20+ year study of hellbenders, *Crytobranchus alleganiensis.* Biol. Conserv. 109:151–156.